Proc. Natl. Acad. Sci. USA
Vol. 90, pp. 1325–1329, February 1993
Biophysics

Pathway of proton transfer in bacterial reaction centers: Second-site mutation Asn-M44 → Asp restores electron and proton transfer in reaction centers from the photosynthetically deficient Asp-L213 → Asn mutant of *Rhodobacter sphaeroides*

(site-directed mutagenesis/bacterial photosynthesis/*Rhodopseudomonas viridis*)

S. H. RONGEY, M. L. PADDOCK, G. FEHER, AND M. Y. OKAMURA

Physics Department, 0319, University of California, San Diego, La Jolla, CA 92093-0319

Contributed by G. Feher, November 9, 1992

ABSTRACT **Site-directed mutagenesis of the photosynthetic reaction center (RC) from *Rhodobacter sphaeroides* has shown Asp-213 of the L subunit (Asp-L213) to be important for photosynthetic viability. Replacement of Asp-L213 with Asn resulted in a photosynthetically deficient mutant, due to the 10^4-fold slower rate for the proton-coupled electron transfer reaction $Q_A^-Q_B^- + 2H^+ \rightarrow Q_AQ_BH_2$ ($k_{AB}^{(2)}$). The detrimental effect of Asn-L213 is surprising since RCs from *Rhodopseudomonas viridis*, *Rhodospirillum rubrum*, and *Chloroflexus aurantiacus* have Asn at the homologous position. However, RCs from these bacteria have an Asp located near Q_B (the secondary quinone acceptor) at the position homologous to Asn-M44 in *Rb. sphaeroides* which might function in place of Asp-L213. To test this conjecture a "*viridis*-like" structure was introduced into *Rb. sphaeroides* by replacing Asp-L213 with Asn and Asn-M44 with Asp. The RCs from this double mutant displayed near-native rates for the electron transfer reaction $k_{AB}^{(2)}$ and restored photosynthetic competence. The rates for the first electron transfer reaction $Q_A^-Q_B \rightarrow Q_AQ_B^-$ ($k_{AB}^{(1)}$) and charge recombination $D^+Q_AQ_B^- \rightarrow DQ_AQ_B$ (k_{BD}) were also restored to near-native values. These results indicate that Asp at *either* the L213 or the M44 site near Q_B can provide a pathway for rapid proton transfer and explain why Asp-L213 need not be conserved in different photosynthetic bacteria. To test further the effect of Asp at M44 on electron and proton transfer to Q_B a mutant containing Asp at *both* L213 and M44 was constructed. The RCs from this mutant (Asn-M44 → Asp) exhibited faster proton-coupled electron transfer to Q_B^-. The increased rate of proton-coupled electron transfer ($k_{AB}^{(2)}$) in the presence of negatively charged Asp residues near Q_B suggests the role of an Asp near Q_B as (*i*) a proton donor group in the proton transfer chain and/or (*ii*) a negatively charged residue stabilizing proton transfer to reduced Q_B.**

In photosynthetic bacteria the reaction center (RC), a membrane-bound pigment–protein complex, converts light energy into chemical energy (see refs. 1 and 2 for review) by catalyzing the transfer of two electrons and two protons to a bound secondary quinone acceptor (Q_B), to form a dihydroquinone (Q_BH_2). The dihydroquinone leaves the RC and helps establish a proton gradient across the plasma membrane that provides the driving force for ATP synthesis.

Recent studies have focused on the pathways and mechanisms of proton transfer to Q_B, which is buried inside the RC. Site-directed mutagenesis of proton donor residues near Q_B has shown three residues, Glu-L212 (3, 4), Ser-L223 (5), and Asp-L213 (4, 6–8), to be important for proton transport in RCs from *Rhodobacter sphaeroides*. Replacement of either Ser-L223 with Ala or Asp-L213 with Asn greatly reduced both the rate of the proton-coupled second electron transfer step, $k_{AB}^{(2)}$ ($Q_A^-Q_B^- + 2H^+ \rightarrow Q_AQ_BH_2$), and the rate of proton uptake. Replacement of Glu-L212 with Gln reduced the rate of proton uptake with little effect on $k_{AB}^{(2)}$. The crystal structure shows Ser-L223 and Asp-L213 to be located near each other (≤3.7 Å), with Ser-L223 forming a hydrogen bond to Q_B (9). A proton transfer pathway to reduced Q_B involving Asp-L213 (4, 6, 7) and Ser-L223 (5, 6) has been proposed (reviewed in ref. 10).

A question about the obligatory role of Asp-L213 in proton transfer arises. Unlike Ser-L223 and Glu-L212, this residue is not conserved in other species of photosynthetic bacteria. For example, RCs from *Rhodopseudomonas viridis* (11) have Asn at L213. However, in *Rb. sphaeroides*, when Asp-L213 is replaced with Asn, effective proton transport is eliminated. Since *Rps. viridis* RCs can function without Asp-L213 a different residue may serve as a proton donor. A candidate for this residue in *Rps. viridis* is Asp-M43. Both this residue in *Rps. viridis* and the homologous Asn-M44 in *Rb. sphaeroides* are close to Q_B (9, 12). Asp-M43 has been implicated in proton transfer in the photosynthetically competent triple mutant (Glu-L212→Ala/Asp-L213→Ala/Asn-M43→Asp) in *Rhodobacter capsulatus* (13).

To determine whether Asp at M44 can replace Asp-L213 in proton transport, RCs from *Rb. sphaeroides* were modified to contain the double mutation Asp-L213 → Asn/Asn-M44 → Asp [DN(L213)/ND(M44)]. The electron and proton transfer rates in this RC were measured and compared with those from native bacteria and the single mutants: DN(L213) (Asp-L213 → Asn) and ND(M44) (Asn-M44 → Asp). The results are interpreted in terms of the functional role of an Asp for proton transport at either the L213 or the M44 site. A preliminary account of this work has been presented (10, 14).

MATERIALS AND METHODS

Site-Directed Mutagenesis. The construction of the site-directed mutants was performed as described (3, 5), with a few modifications as noted. An oligonucleotide was synthesized to direct the mutagenesis of Asp-L213 → Asn: 5′-GATCACGAGAACACGTTCTTCC-3′; the AAC codon for Asn replaced the native GAT codon for Asp-L213. For the replacement of Asn-M44 with Asp, the oligonucleotide 5′-TGGTTCGGCGACGCCCAGCT-3′ was used to replace the native AAC codon for Asn-M44 with the GAC Asp codon. The mutation at L213 was incorporated into an M13 phage vehicle containing the *Pvu* II–*Sal* I fragment (482 bp) which contains the DNA coding for the latter half of the L subunit

The publication costs of this article were defrayed in part by page charge payment. This article must therefore be hereby marked "*advertisement*" in accordance with 18 U.S.C. §1734 solely to indicate this fact.

Abbreviations: D, primary donor; Q_A, primary quinone acceptor; Q_B, secondary quinone acceptor; QH_2, dihydroquinone; RC, reaction center; Cyt, cytochrome.

(5). The mutation at M44 was incorporated into an M13 vehicle containing the *Sal* I–*Bam*HI fragment (988 bp) which contains the entire gene coding for the M subunit (*pufM*) (a *Bam*HI site was introduced just after *pufM*). The sequences around each mutation showed no other changes in the subcloned regions. The mutated DNA sequences were introduced into a pRK vector containing the reconstructed *puf* operon (3, 5). The mutations in *pufM* required the construction of an intermediate vector. First, *pufM*, with the ND(M44) mutation, was moved into the pBC SK(+) plasmid (Stratagene). Then *pufL* [from either native or DN(L213) mutant] was inserted, reconstructing the *pufL* and *pufM* of the *puf* operon. The mutant *puf* operons were transferred into the *Rb. sphaeroides* deletion strain ΔLM1 (5).

Photosynthetic Growth Tests. Photosynthetic viability was tested both in liquid cultures and on plates. Liquid cultures were grown anaerobically (incandescent lighting, 25 mW/cm^2; 33°C) to apply photosynthetic selection to the cultures. To determine the growth rate, cell density was monitored by scattering at 680 nm [Spectronic 20 spectrophotometer (Bausch & Lomb)]. An alternative test of photosynthetic viability was to determine the fraction of bacteria that could grow photosynthetically on solid medium. Aliquots containing 10^3, 10^5, or 10^8 bacterial cells from aerobic liquid cultures in logarithmic phase were spread onto duplicate plates. One plate was incubated anaerobically to allow only photosynthetically competent cells to grow [GasPak 100 or the 150 Jar system (Baltimore Biological Laboratory)]. The chamber was placed in a water bath (33°C) surrounded by 12–14 incandescent lights (40-W bulbs 10 cm from the chamber) and purged with dry N_2 prior to use. The duplicate plate was grown aerobically to determine the total number of viable cells.

RC Preparation. RCs were isolated from semi-aerobically grown cells by using *N,N*-dimethyldodecylamine-*N*-oxide (Fluka Chemie) as described (15); the purified RCs had an A_{280}/A_{802} ratio < 1.3. Q_B was reconstituted as described (5). Special precautions were taken with DN(L213) RCs to reduce the accumulation of the charge-separated state ($D^+Q_AQ_B^-$, where D is the primary electron donor), which was exceptionally stable at pH <8 (see *Results and Analysis*). To reconstitute the mutant RCs with Q_B, they were dialyzed against 2 mM Tris at pH 9 [instead of 2 mM Hepes (Calbiochem) at pH 7.5]. Ferricyanide (20 μM) was added to reduce (from ≈80% to ≤10%) the amount of $DQ_AQ_B^-$ present in the dark.

Electron Transfer and Proton Uptake Rate Measurements. The kinetics of the absorption changes accompanying electron transfer were recorded on a modified Cary 14 spectrophotometer (Varian) as described (16). All measurements were performed at 23°C as described (3, 5) (see figure captions for conditions). The proton uptake was measured under the same conditions as the electron transfer $k_{AB}^{(2)}$ except that the buffer was omitted and 50 μM phenol red was added.

RESULTS AND ANALYSIS

Photosynthetic Growth. The photosynthetic growth of the complemented deletion strains carrying the native or the mutated *puf* operons (containing the L and M genes) was tested in both liquid cultures and on plates. The doubling time of the native strain was 3–4 hr in liquid culture. The DN(L213) strain showed no growth for a few days; however, growth was occasionally observed after 3–4 days due to spontaneous photosynthetic reversions. The photosynthetic growth of the strains carrying the DN(L213)/ND(M44) and ND(M44) mutations was similar to that of the native strain, with a doubling time of 3–4 hr and no lag period.

Growth studies using plates confirmed that the DN(L213) strain was photosynthetically deficient. The ratio of colonies on the anaerobic (photosynthetically viable cells) and aerobic (all viable cells) plates was 1.0 ± 0.1 for the strains carrying the native or ND(M44) genes, but only ≈10^{-6} for the DN(L213) strain (Fig. 1). This small fraction of photosynthetically competent cells reflects the frequency of spontaneous mutations compensating for the Asp-L213 → Asn lesion. The ratio was restored to near 1 (0.9 ± 0.2) for the double mutant DN(L213)/ND(M44) strain, showing the compensating effect of the Asn-M44 → Asp mutation. Thus, the Asp-L213 → Asn mutation inhibits photosynthetic growth, which is restored by the second-site mutation Asn-M44 → Asp.

Electron and Proton Transfer Rates. The lack of photosynthetic growth in the strain carrying the Asp-L213 → Asn mutation suggests that some electron and/or proton transfer rate has been decreased in the RC. To test which of these transfer steps were affected by the mutations, the rate of each of them was measured. The electron transfer reactions involving Q_B are shown in Eqs. 1 and 2.

$$DQ_AQ_B \xrightarrow[h\nu]{Cyt^{2+} \rightarrow Cyt^{3+}} DQ_A^-Q_B \xrightarrow{k_{AB}^{(1)}} DQ_AQ_B^- \quad [1]$$

$$DQ_AQ_B^- \xrightarrow[h\nu]{Cyt^{2+} \rightarrow Cyt^{3+}} DQ_A^-Q_B^- + 2H^+ \xrightarrow{k_{AB}^{(2)}} DQ_AQ_BH_2 \quad [2]$$

The first electron is transferred from the reduced primary quinone Q_A^- to Q_B, with rate constant $k_{AB}^{(1)}$ (Eq. 1). The second electron is transferred to Q_B with rate constant $k_{AB}^{(2)}$ (Eq. 2), which involves the binding of two protons to form the dihydroquinone Q_BH_2. The dihydroquinone leaves the RC and is replaced by an exogenous quinone. This restores the initial state DQ_AQ_B and completes the cycle. For each electron transferred to the quinones from the donor (D), one cytochrome (Cyt) is oxidized providing a measure of the overall RC cycle rate. The overall rate of Cyt oxidation, the rates $k_{AB}^{(1)}$ and $k_{AB}^{(2)}$, the proton uptake from solution, and the charge recombination rates k_{AD} ($D^+Q_A^- \rightarrow DQ_A$) and k_{BD} ($D^+Q_AQ_B^- \rightarrow DQ_AQ_B$) were measured in native and mutant RCs. These rates (at pH 7.5) are summarized in Table 1.

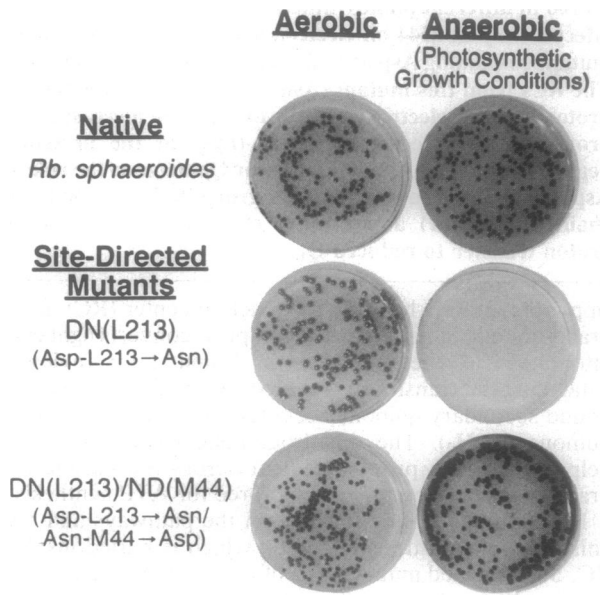

FIG. 1. Assay for photosynthetic competence of native and site-directed mutants of *Rb. sphaeroides*. Equal numbers of cells (≈100) were grown under aerobic and anaerobic (i.e., photosynthetic) conditions. The DN(L213) mutant is photosynthetically deficient. Photosynthetic competence was restored in the DN(L213)/ND(M44) mutant, showing that Asp-M44 can compensate for the removal of Asp-L213.

Table 1. Electron and proton transfer rates for native and mutant RCs at pH 7.5

	Native*	DN(L213)	DN(L213)/ ND(M44)	ND(M44)
Rate constants, s^{-1}				
k_{AD}	10	10	12	8
k_{BD}	0.8	0.05	0.5	3
$k_{AB}^{(1)}$	6800	350	2000	1800
$k_{AB}^{(2)}$	1500	0.25	1200	8000
k_{H^+}	1300	0.23	1000	—†
Cyt oxidation‡				
Fast	>5	1.9 ± 0.1	>5	>5
Steady state	1000	0.4	700	400
Photosynthetic competence	+	−	+	+

Variations between RC preparations were typically within ±10% for all measurements.

**Rb. sphaeroides* strain 2.4.1 or R26; no differences between strains were observed.

†Proton uptake due to proton transfer to Q_B was not resolvable from other events (e.g., proton release accompanying the formation of D^+) on the 100-μs time scale.

‡See Fig. 2. The number of Cyt molecules oxidized indicates the number of electrons transferred to the quinones. A maximum of 3 (Cyt/RC) can be oxidized (forming $Q_A^-Q_B^-$) without turnover of Q_B. The photocycle of DN(L213) is blocked after two electrons are taken up by the RC (forming $Q_A^-Q_B^-$). The steady-state rate, (cyt/RC)s^{-1}, equals twice the photocycle rate (see Eqs. 1 and 2).

Cyt Oxidation. The Cyt oxidation rate was measured at pH 7.5 by monitoring ΔA_{550} while illuminating RCs in the presence of excess horse heart cyt *c* and ubiquinone 50. In native RCs the oxidation rate was 1000 Cyt *c* molecules per RC per second [(Cyt/RC)s^{-1}]. The DN(L213) RCs showed a rapid oxidation of 1.9 ± 0.1 (Cyt/RC)s^{-1} followed by a steady-state turnover rate of 0.4 (cyt/RC)s^{-1} (Fig. 2), as reported earlier (6). In the double mutant DN(L213)/ND(M44) the cytochrome oxidation rate was restored to 700 (cyt/RC)s^{-1}. For the ND(M44) RCs the rate was 400 (cyt/RC)s^{-1}. This slower rate was not due to slower electron transfer (see below) and may have been due to weaker quinone binding.

The decreased Cyt oxidation rate for the DN(L213) RCs and the near-native Cyt oxidation rate for DN(L213)/ND(M44) and ND(M44) RCs correlates with photosynthetic competence. These results suggest that a specific electron and proton transfer step is impaired by the single Asp-L213 → Asn mutation, which can be restored by the compensating change Asn-M44 → Asp.

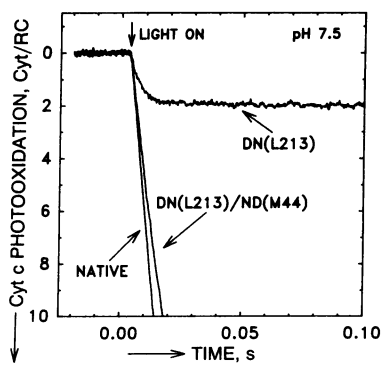

FIG. 2. Cyt photooxidation by native, DN(L213), and DN(L213)/ND(M44) RCs. The photooxidation of Cyt *c* was monitored at 550 nm in the presence of exogenous quinone and Cyt c under continuous illumination. (Conditions: 0.7–1.0 μM RCs/20–35 μM Cyt c/10 mM Hepes, pH 7.5/either 0.025% sodium deoxycholate or 0.04% dodecyl β-D-maltoside/50 mM KCl; 1 W/cm, 23°C, λ = 550 nm.) The Asp-L213→Asn mutation drastically reduced the turnover rate (following a rapid oxidation of 2 Cyt/RC). The second mutation (Asn-M44 → Asp) in the DN(L213)/ND(M44) RCs restored the Cyt turnover to near native values.

First Electron Transfer. The rate constant $k_{AB}^{(1)}$ (Eq. 1) was measured by monitoring the electrochromic shift of bacteriopheophytin at 750.5 nm following reduction of Q_A (16, 17). For native RCs, $k_{AB}^{(1)}$ was 6800 s^{-1} at pH 7.5. The rate was ≈20 times slower for DN(L213) RCs but only 3–5 times slower for DN(L213)/ND(M44) and ND(M44) RCs (Table 1).

The pH dependence of $k_{AB}^{(1)}$ is shown in Fig. 3. Native and DN(L213)/ND(M44) RCs have an approximately constant $k_{AB}^{(1)}$ below the turning point near pH 8, with the DN(L213)/ND(M44) rates about 5 times slower than the native rates. The turning point has been attributed to the titration of Glu-L212 (3, 4). That it occurs near the same pH suggests that the electrostatic environment near Glu-L212 is the same in both RCs. In contrast, the DN(L213) RCs displayed a much slower $k_{AB}^{(1)}$ with a linear dependence on proton concentration. ND(M44) mutant RCs showed no pH dependence over the range 5.4–8.8 (data not shown).

Second Electron Transfer. The rate constant $k_{AB}^{(2)}$ (Eq. 2) was measured by monitoring the disappearance of semiquinone at 450 nm after two laser flashes in the presence of exogenous donors (17). In native RCs the semiquinone signal decayed after the second flash, concomitant with the disappearance of $Q_A^-Q_B^-$, corresponding to $k_{AB}^{(2)}$ = 1500 s^{-1} at pH 7.5. In DN(L213) RCs the rate was drastically reduced to 0.25 s^{-1}, as previously reported (4, 6, 7). In the double-mutant DN(L213)/ND(M44) RCs, $k_{AB}^{(2)}$ was restored to values near those of native RCs (Table 1). These results show that Asp-M44 can take over the function of Asp-L213 in this reaction. In ND(M44) RCs, $k_{AB}^{(2)}$ was *faster* (8000 s^{-1}) than in native RCs.

The pH dependence of $k_{AB}^{(2)}$ is shown in Fig. 4. Both the native and DN(L213)/ND(M44) RCs have turning points near pH 8. That $k_{AB}^{(1)}$ and $k_{AB}^{(2)}$ in the double-mutant RCs reach approximately the same plateau at low pH may either be fortuitous or indicate the same rate-limiting process [e.g., a conformational change (18) or an internal proton transfer between amino acid residues] for both electron transfers. The rates in the DN(L213) RCs were much slower and showed a linear dependence on proton concentration. The rates in the ND(M44) RCs were 4- to 8-fold faster than native from pH 5.0 to 8.3 (data not shown).

Proton Uptake. Proton uptake from solution was determined by monitoring ΔA_{557} of the pH indicator dye phenol red (5, 19). For the DN(L213) mutant the proton uptake rates following two laser flashes exhibited a slow phase with a rate of 0.23 s^{-1} at pH 7.5. This rate is the same as $k_{AB}^{(2)}$ and the photocycle rate (see footnote ‡ of Table 1), showing that all three reactions are limited by the same process. Both native and DN(L213)/ND(M44) RCs had fast proton uptake rates—1300 and 1000 s^{-1}, respectively—showing that Asp at either M44 or L213 is

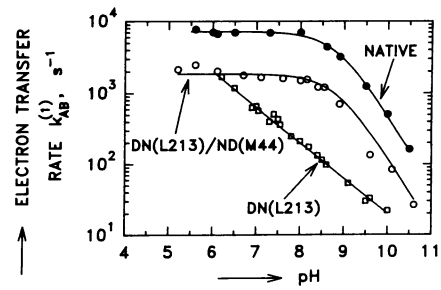

FIG. 3. pH dependence of the electron transfer rate constant $k_{AB}^{(1)}$ (see Eq. 1) for native, DN(L213), and DN(L213)/ND(M44) RCs. The pH profiles of the native and double mutant are similar, whereas the DN(L213) mutant displays an altered pH profile. (Conditions: 3–5 μM RCs/2 mM each Hepes, Caps, Ches, Mes, Pipes, and Tris/0.04% dodecyl β-D-maltoside/50 mM KCl; 23°C; λ = 750.5 nm.)

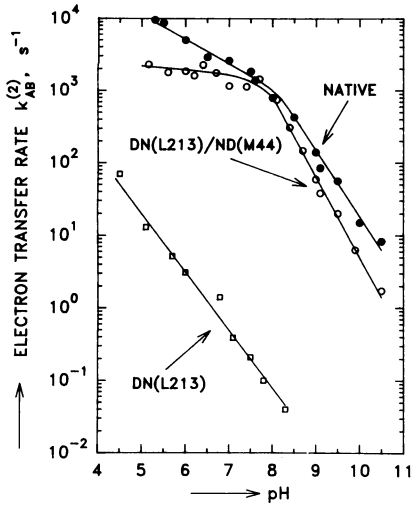

FIG. 4. pH dependence of the electron transfer rate constant $k_{AB}^{(2)}$ for the reaction $Q_A^-Q_B^- + 2H^+ \rightarrow Q_AQ_BH_2$, for native, DN(L213), and DN(L213)/ND(M44) RCs. Note the drastic reduction of the transfer rate in the DN(L213) mutant. The transfer rate was restored by the compensating mutation in the DN(L213)/ND(M44) mutant. (Conditions: same as in Fig. 3 except 1–3 μM RCs/20–600 μM ferrocene or 20–50 μM Cyt *c* and λ = 450 nm.)

effective in proton transfer (data not shown). Proton uptake by ND(M44) RCs was not resolved (see footnote † of Table 1).

Charge Recombination. Charge recombination serves as a useful probe for determining energy difference between the $Q_A^-Q_B$ and $Q_AQ_B^-$ states (16). The charge-recombination rate constants k_{AD} ($D^+Q_A^- \rightarrow DQ_A$) and k_{BD} ($D^+Q_AQ_B^- \rightarrow DQ_AQ_B$) were measured by monitoring the recovery of the oxidized donor at 865 nm following a laser flash. k_{AD} was measured in RCs containing only Q_A or in RCs in the presence of 200 μM terbutryne, which displaces Q_B (15). In native, DN(L213), and DN(L213)/ND(M44) RCs the rates were similar, with $k_{AD} \approx 10\ s^{-1}$, and essentially independent of pH (data not shown).

The rate constant k_{BD} was measured in RCs in the presence of excess ubiquinone 50, to maximize Q_B occupancy. In native RCs k_{BD} was 0.8 s^{-1}, whereas in DN(L213) RCs k_{BD} was reduced to 0.05 s^{-1} (pH 7.5), indicating that the Asp-L213 → Asn mutation stabilizes the charge-separated state ($D^+Q_AQ_B^-$) (7). At pH 7.5, k_{BD} was similar to that of native RCs for DN(L213)/ND(M44) (0.5 s^{-1}) and faster than native RCs for ND(M44) (3 s^{-1}).

The pH dependence of k_{BD} was measured from pH 5 to pH 11 (Fig. 5). Compared with native RCs, k_{BD} was 5–10 times slower in DN(L213) RCs, 2–8 times faster in ND(M44) RCs (data not shown), and about the same in DN(L213)/ND(M44) RCs.

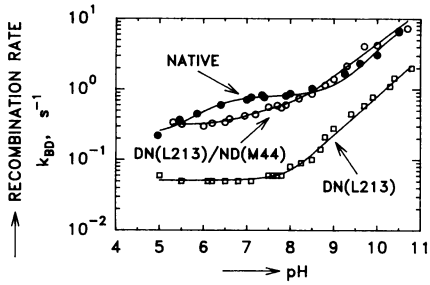

FIG. 5. Charge recombination rate k_{BD}, for the reaction $D^+Q_AQ_B^- \rightarrow DQ_AQ_B$, as a function of pH for native, DN(L213), and DN(L213)/ND(M44) RCs. The DN(L213) RCs show a decreased rate—i.e., increased stability of the $D^+Q_AQ_B^-$ state—at all pH. (Conditions: same as in Fig. 3 except ≈2 μM RCs and λ = 865 nm.)

DISCUSSION

The second-site mutation Asn-M44 → Asp restored near-native proton and electron transfer rates to the functionally deficient Asp-L213 → Asn RC from *Rb. sphaeroides*. The rate of the proton-coupled second electron transfer reaction, $k_{AB}^{(2)}$ (Fig. 4), and the rate of proton uptake (Table 1) in RCs from the DN(L213)/ND(M44) double mutant were increased by 3–4 orders of magnitude compared with DN(L213) RCs, consistent with the restoration of a proton pathway by the Asn-M44 → Asp mutation.

Lack of Conservation of Asp at L213 or M44. The ability of RCs containing Asp at either L213 or M44 to sustain high rates of electron and proton transfer can account for the lack of conservation of Asp at L213 or M44 in RCs from photosynthetic bacteria. The alignment of RC sequences from different strains of photosynthetic bacteria (Fig. 6) shows that all bacterial RCs contain an Asp at *either* L213 or M44. RCs from *Rb. sphaeroides* (20, 21), *Rb. capsulatus* (22), and *Erythrobacter* sp. OCH114 (23) have an Asp at position L213, and an Asn at M44. RCs from *Rps. viridis* (11), *Rs. rubrum* (24), and *C. aurantiacus* (25, 26) have Asn at L213 and Asp at M44. Thus, the results presented here support the hypothesis that Asp residues at L213 or M44 serve the same function in different bacterial species. Hanson *et al.* (13) have proposed the same role for Asp-M43 in *Rps. viridis*, based on work in *Rb. capsulatus*. In their work photosynthetic competence was restored to the double mutant Glu-L212 → Ala/Asp-L213 → Ala by a spontaneous mutation of Asn-M43 to Asp.

Proton Transfer Pathways to Q_B. Proton transfer from aqueous solution to the buried Q_B molecule must be mediated by residues of the RC since Q_B does not have direct solvent accessibility. In the x-ray crystal structure of the region around Q_B in the RC from *Rb. sphaeroides* (9) (Fig. 7), quinone is hydrogen-bonded to Ser-L223 and His-L190. Residues Asp-L213 and Asn-M44 are located near Ser-L223 and Q_B. A proton transfer pathway to Q_B has been proposed for native RCs, based on results from mutations that slow both the $k_{AB}^{(2)}$ and cytochrome turnover rates. Both Ser-L223 (5) and Asp-L213 (refs. 6 and 7; see refs. 10 and 14 for review) are important for proton transfer to Q_B. Asp-L213 is connected to solvent through the nearby Asp-L210 and Arg-L217, completing the proton pathway. Asp introduced at M44 must compensate for the loss of Asp at L213 in the DN(L213)/ND(M44)

Photosynthetic Bacteria	Amino Acid Sequences	
	L213	M44
Rb. sphaeroides	P D H E [D] T F F R	G W F G [N] A Q L G
Rb. capsulatus	P D H E [D] T Y F R	G W M G [N] A Q I G
E. sp. OCH114	P D H E [D] T F F R	G L F G [N] G Q I G
Rps. viridis	A E H E [N] Q Y F R	G K I G [D] A Q I G
Rs. rubrum	P E H E [N] T Y F Q	G K I G [D] A Q I G
C. aurantiacus	G D I E [N] V F F R	N F G F [D] S Q L G
Site-Directed Mutants (*Rb. sphaeroides*)		
DN(L213)	P D H E [N] T F F R	G W F G [N] A Q L G
DN(L213)/ND(M44)	P D H E [N] T F F R	G W F G [D] A Q L G
ND(M44)	P D H E [D] T F F R	G W F G [D] A Q L G

FIG. 6. Sequence alignments of the L213 and M44 regions of *Rb. sphaeroides* (20, 21) and the analogous region of five other photosynthetic bacteria (numbering corresponds to *Rb. sphaeroides*): *Rb. capsulatus; Erythrobacter* sp. OCH114, *Rps. viridis, Rhodospirillum rubrum*, and *Chloroflexus aurantiacus*. All the species maintain an Asp residue at either the site analogous to L213 or that analogous to M44. In *Rb. sphaeroides* both Asp-L213 and Asn-M44 are near Ser-L223, which has been implicated in proton transfer to Q_B (5). The introduction of an Asp at M44 creates an alternative proton pathway leading to Ser-L223 and Q_B (see Fig. 7).

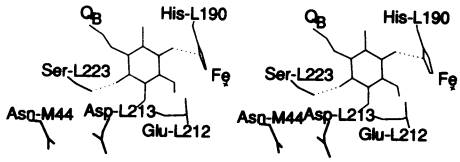

FIG. 7. Stereo view of the Q_B binding pocket (coordinates from ref. 9). For simplicity only the side chains of the amino acids are shown. Ser-L223 and His-L190 are hydrogen-bonded (dotted lines) to the carbonyl oxygens of Q_B. The oxygen of Asp-L213 and the oxygen or nitrogen of Asn-M44 are 4.3 and 6.7 Å, respectively, from the carbonyl oxygen of Q_B and 3.7 Å and 5.5 Å, respectively, from the Ser-L223 hydroxyl oxygen.

mutant. In contrast to Asp-L213, Asn-M44 has direct solvent accessibility (P. Beroza, personal communication) but is farther from both Ser-L223 (5.5 vs. 3.7 Å) and Q_B (6.7 vs. 4.3 Å). The larger distance between Asp-M44 [in DN(L213)/ND(M44) RCs] and Ser-L223 or Q_B seems to rule out a direct proton transfer. However, proton transfer could involve an internal water molecule. A bound water molecule was found in *Rps. viridis* between Asp-M43 (homologous to M44 in *Rb. sphaeroides*) and Ser-L223 (12). Thus, Asp at M44 opens up a new proton transfer pathway from the solvent to Q_B.

Mechanism of Proton Transfer. The slow rate of electron and proton transfer in RCs lacking Asp at both the L213 and M44 sites [DN(L213) mutant] has been attributed to a blockage in the proton transfer pathway to Q_B (4, 6, 7). The blockage could be a consequence of two effects: (*i*) the mutation removes a proton donor group from the transfer pathway; (*ii*) replacement of the negatively charged Asp-L213 with the neutral Asn increases the electrostatic energy for proton transfer to Q_B^-.

To determine which of these mechanisms predominates, we need an assay for the electrostatic energy of Q_B^-. Charge recombination (k_{BD}) provides such an assay, since this rate is sensitive to the free-energy difference between the $Q_A^-Q_B$ and $Q_AQ_B^-$ states (16).

Evidence that Asp-L213 is a component of a proton donor chain comes from a comparison between the kinetics of two mutants: DN(L213) (Asp-L213 → Asn) and DE(L213) (Asp-L213 → Glu) (ref. 14; unpublished work). The recombination rate k_{BD} is approximately the same in both mutants, implying similar electrostatic environments for Q_B^- in both mutants (Glu-L213 presumably is protonated). Yet, $k_{AB}^{(2)}$ is 30-fold faster in the DE(L213) mutant than in the DN(L213) mutant. Since the electrostatic environment of Q_B^- is essentially the same in both mutants, the increase in $k_{AB}^{(2)}$ is presumably due to Glu-L213, which is a better proton donor than Asn-L213. Additional evidence of the function of Asp-L213 as a proton donor comes from the effect of weakly acidic substances such as azide, which can act as proton carriers, in increasing $k_{AB}^{(2)}$ in the DN(L213) mutant (8).

In contrast to the two mutations discussed above, the electrostatic environment of Q_B^- in the DN(L213) mutant has been altered from that of the native environment. The observed reduction of k_{BD} in DN(L213) RCs, relative to native RCs, is consistent with the removal of a negative charge near Q_B (7). In the DN(L213)/ND(M44) RCs, k_{BD} was restored to values similar to those observed in native RCs, showing that the charge on Asp is equally effective at L213 and M44 in destabilizing the Q_B^- state. In RCs containing Asp at both L213 and M44 [ND(M44)], k_{BD} was faster than in native RCs, indicating a further destabilization of Q_B^- due to the larger negative charge near Q_B. The faster $k_{AB}^{(2)}$, beyond that expected for two parallel pathways, in these RCs suggests that a net negative charge near Q_B is important for the proton-coupled second electron transfer.

The importance of negatively charged residues (Asp-L213 and/or Asp-M44) near Q_B in functionally active RCs suggests an important electrostatic role of these residues in proton transport, apart from their proposed role as proton donors. The negatively charged Asp could stabilize proton uptake to the interior of the RC by reducing the potential energy of other donor residues along the proton transfer pathway. For example, removing a negative charge near Q_B could decrease the pK_a of a group (even possibly Q_BH), which could decrease the second electron transfer rate if its protonation is required for electron transfer. Further experiments are necessary to delineate the relative importance of the electrostatic contribution and proton donor functions of various residues in native and mutant RCs.

We thank Ed Abresch for purification of the RCs, Paul McPherson for the proton uptake measurements, and Andrea Juth for technical assistance. This work was supported by grants from the National Institutes of Health (GM13191, GM41637, 2T32DK07233-16) and the National Science Foundation (DMB89-15631).

1. Feher, G., Allen, J. P., Okamura, M. Y. & Rees, D. C. (1989) *Nature (London)* **339**, 111–116.
2. Cramer, W. A. & Knaff, D. B. (1990) *Energy Transduction in Biological Membranes* (Springer, New York).
3. Paddock, M. L., Rongey, S. H., Feher, G. & Okamura, M. Y. (1989) *Proc. Natl. Acad. Sci. USA* **86**, 6602–6606.
4. Takahashi, E. & Wraight, C. A. (1992) *Biochemistry* **31**, 855–866.
5. Paddock, M. L., McPherson, P. H., Feher, G. & Okamura, M. Y. (1990) *Proc. Natl. Acad. Sci. USA* **87**, 6803–6807.
6. Rongey, S. H., Paddock, M. L., Juth, A. L., McPherson, P. H., Feher, G. & Okamura, M. Y. (1991) *Biophys. J.* **59**, 142a (abstr.).
7. Takahashi, E. & Wraight, C. A. (1990) *Biochim. Biophys. Acta* **1020**, 107–111.
8. Takahashi, E. & Wraight, C. A. (1991) *FEBS Lett.* **283**, 140–144.
9. Allen, J. P., Feher, G., Yeates, T. O., Komiya, H. & Rees, D. C. (1988) *Proc. Natl. Acad. Sci. USA* **85**, 8487–8491.
10. Okamura, M. Y. & Feher, G. (1992) *Annu. Rev. Biochem.* **61**, 861–896.
11. Michel, H., Weyer, K. A., Gruenberg, H., Dunger, I., Oesterhelt, D. & Lottspeich, F. (1986) *EMBO J.* **5**, 1149–1158.
12. Deisenhofer, J. & Michel, H. (1989) *EMBO J.* **8**, 2149–2170.
13. Hanson, D. K., Nance, S. L. & Schiffer, M. (1992) *Photosynth. Res.* **32**, 147–153.
14. Okamura, M. Y., Paddock, M. L., McPherson, P. H., Rongey, S. & Feher, G. (1992) *Research in Photosynthesis*, ed. Murata, N. (Kluwer, Dordrecht, The Netherlands), in press.
15. Paddock, M. L., Rongey, S. H., Abresch, E. C., Feher, G. & Okamura, M. Y. (1988) *Photosynth. Res.* **17**, 75–96.
16. Kleinfeld, D., Okamura, M. Y. & Feher, G. (1984) *Biochim. Biophys. Acta* **766**, 126–140.
17. Vermeglio, A. & Clayton, R. K. (1977) *Biochim. Biophys. Acta* **461**, 159–165.
18. Brzezinski, P., Okamura, M. Y. & Feher, G. (1992) in *Proceedings of the NATO Workshop in Structure, Function and Dynamics of the Bacterial Reaction Center*, Cadarache, France, May 10–15, 1992, ed. Breton, J. (Plenum, New York), in press.
19. Wraight, C. A. (1979) *Biochim. Biophys. Acta* **548**, 309–327.
20. Williams, J. C., Steiner, L. A., Ogden, R. C., Simon, M. I. & Feher, G. (1983) *Proc. Natl. Acad. Sci. USA* **80**, 6505–6509.
21. Williams, J. C., Steiner, L. A., Feher, G. & Simon, M. I. (1984) *Proc. Natl. Acad. Sci. USA* **81**, 7303–7307.
22. Youvan, D. C., Bylina, E. J., Alberti, M., Begusch, H. & Hearst, J. E. (1984) *Cell* **37**, 949–957.
23. Liebetanz, R., Hornberger, U. & Drews, G. (1991) *Mol. Microbiol.* **5**, 1459–1468.
24. Bélanger, G., Bérard, J., Corriveau, P. & Gingras, G. (1988) *J. Biol. Chem.* **263**, 7632–7638.
25. Ovchinnikov, Y. A., Abdulaev, N. G., Zolotarev, A. S., Shmuckler, B. E., Zargarov, A. A., Kutuzov, M. A., Telezhinskaya, I. N. & Levina, N. B. (1988) *FEBS Lett.* **231**, 237–242.
26. Ovchinnikov, Y. A., Abdulaev, N. G., Shmuckler, B. E., Zargarov, A. A., Kutuzov, M. A., Telezhinskaya, I. N., Levina, N. B. & Zolotarev, A. S. (1988) *FEBS Lett.* **232**, 364–368.